Electronic Supporting Information

Oxygen Reduction Using a Metal-Free Naphthalene Diimide-Based Covalent Organic Framework Electrocatalyst

Sergio Royuela,[‡a,b] Emiliano Martínez-Periñán,[‡c] Marina P. Arrieta,[a] José I. Martínez,[d] M. Mar Ramos,[b] Félix Zamora,*[e,f,g,h] Encarnación Lorenzo*[c,f,g] and José L. Segura*[a]

[a] Departamento de Química Orgánica I, Facultad de CC. Químicas, Universidad Complutense de Madrid, 28040 Madrid, Spain.

[b] Departamento de Tecnología Química y Ambiental, Universidad Rey Juan Carlos, 28933 Madrid, Spain.

[c] Departamento de Química Analítica y Análisis Instrumental, Facultad de Ciencias, Universidad Autónoma de Madrid, 28049 Madrid, Spain.

[d] Departamento de Nanoestructuras, Superficies, Recubrimientos y Astrofísica Molecular, Instituto de Ciencia de Materiales de Madrid (ICMM-CSIC), 28049 Madrid, Spain.

[e] Departamento de Química Inorgánica, Facultad de Ciencias, Universidad Autónoma de Madrid, 28049 Madrid, Spain.

[f] Instituto Madrileño de Estudios Avanzados en Nanociencia (IMDEA-Nanociencia), Cantoblanco, 28049 Madrid, Spain.

[g] Institute for Advanced Research in Chemical Sciences (IAdChem), Universidad Autónoma de Madrid, 28049 Madrid, Spain.

[h] Condensed Matter Physics Center (IFIMAC), Universidad Autónoma de Madrid, 28049 Madrid, Spain.

‡ These authors contributed equally to this work.

General Methods

Thin layer chromatography (TLC) was performed using pre-coated silica gel 60 F254 and compounds were visualized under UV light (λ = 254 nm). Solution ^{1}H NMR and ^{13}C NMR spectra were recorded on a Bruker AVIII-300 MHz spectrometer. Chemical shifts were reported in ppm and referenced to the residual non-deuterated solvent frequencies ($CDCl_3$: δ 7.26 ppm for ^{1}H, 77.0 ppm for ^{13}C). Mass spectra were recorded by means of matrix-assisted laser desorption/ionization time-of-flight (MALDI-TOF) or fast atom bombardment (FAB) ionization techniques.

Materials

The following reagents were commercially available and were used as received: 1,4,5,8-naphthalenetetracarboxylic dianhydride (NTCDA), p-nitroacetophenone, trifluoromethane-sulfonic acid, palladium on carbon (10 wt%), hydrazine hydrate (50-60 wt%), platinum on carbon (10 wt%).
1,3,5-tris-(4-aminophenyl)benzene (TAPB)[1] and *N,N'*-bis-(2-ethylhexyl)-1,4,5,8-naphthalene-tetracarboxydiimide (NDI-monomer)[2] were prepared according to previously reported procedures.

Instrumental

- Fourier-transform infrared spectroscopy (FTIR). Solids were analysed by FTIR on a Bruker TENSOR 27 on a diamond plate (ATR).

- Powder X-ray diffraction (PXRD). PXRD measurements were carried out with X'PERT MPD with conventional Bragg-Brentano geometry using monochromatic Cu Kα1 radiation (λ = 1.5406 Å) in the 2θ = 2° - 40° range.

- Solid state ^{13}C cross-polarization magic angle spinning NMR (13C-CP/MAS-NMR). ^{13}C CP/MAS NMR spectra were recorded on a Bruker AVANCE III HD-WB 400 MHz with a rotation frequency of 12 kHz.

- N_2 sorption isotherms. N_2 (77 K) adsorption-desorption measurements were carried out on a Micromeritics Tristar 3000. Samples were previously activated for 4 h under high vacuum ($<10^{-7}$ bar) at 120 °C.

- Thermogravimetric analysis (TGA). TGA was performed on a TGA-Q50 instrument on a platinum plate, heating the samples under nitrogen atmosphere at a heating rate of 10 °C/min.

- Dynamic light scattering (DLS). DLS studies were carried out using a Vasco 1 particle size analyser of Cordouan Technologies.

- Transmission electron microscopy (TEM). TEM micrographs and the corresponding selected area electron diffraction (SAED) patterns were recorded in a JEOL JEM 2100 TEM at 200 kV.

- Atomic force microscope (AFM). AFM was used in dynamic mode using a Nanotec Electronica system operating at room temperature under ambient air conditions. The obtained images were processed using WSxM (freely downloadable scanning probe microscopy software from www.nanotec.es).[3] For AFM measurements, commercial Olympus Si/N and Ti/Pt cantilevers were used with a nominal force constant of 0.75 N/m and 2 N/m, respectively. The surfaces used for AFM experiments were SiO_2 (300 nm thickness)/Si (IMS Company).

- AFM sample preparation. Freshly prepared water **NDI-COF** colloids were deposited by drop-casting on SiO_2 and after 30 min dried under an Argon flow. SiO_2 surfaces were previously sonicated for 15 min in acetone, 15 min in 2-propanol and then dried under an Argon flow.

- Electrochemical measurements were carried out with a Bipotentiostat PGSTAT302N MBA (Metrohm Autolab) using the software package NOVA 1.11 (Metrohm Autolab). Static electrochemical measurements were carried out on a glass and Teflon homemade cell. Glassy Carbon (GC) electrodes (0.07 cm^2 Ø with an electrochemical area of 0.1 cm^2) from CH Instruments were used as working electrodes, Pt wire as counter electrode and a homemade calomel electrode as reference electrode. Rotating disk-ring electrode (RRDE) measurements were carried out using a glassy carbon disk/platinum ring RRDE electrode from PINE and the same counter and reference electrode as in static measurements. A modulated speed rotator from PINE Instruments was used and measures were carried out in a commercial electrochemical cell adapted to rotating disc electrodes.

The GC electrodes modification was carried out by drop-casting 80 µL of the **NDI-CON** suspension and letting it dry at room temperature. 5 µL of 1 mg/mL platinum on carbon (10 wt%) in 20% EtOH, 0.02% Nafion ink were drop-casted over the GC electrodes and allowed to dry at room temperature. Suspensions of 1 mg of **NDI-polymer** and NDI-monomer in 5 mL of Milli Q water were prepared and sonicated for 2h. 80 µL of each suspension were then drop-casted over the disc of a GC disc/ Pt ring RRDE.

A 15x15 mm cylindrical graphite SEM mount has been used to take the SEM images of **NDI-CON** before and after electrocatalyst. The **NDI-CON** modified graphite mount (80 µL of **NDI-CON** suspension in an area around 0.1 cm^2) was used as working electrode, and a potential of -0.5 V *vs.* calomel electrode was applied with the electrode surface immersed in a O_2 saturated 0.1 M NaOH solution for 3000 seconds.

HOPG plates were modified with 80 µL of an **NDI-CON** suspension in an area of around 0.1 cm^2 and an AFM study of their topography before and after electrocatalyst was performed. The modified **NDI-CON** HOPG plate was used as working electrode immersed in an O_2 saturated 0.1 M NaOH solution, applying a potential of -0.5 V *vs.* calomel electrode for 3000 seconds.

Synthesis

- **NDI-COF**: In a pyrex tube NTCDA (40.2 mg, 0.15 mmol) and TAPB (35.1 mg, 0.1 mmol) were suspended in a mixture of *N*-methyl-2-pyrrolidone (NMP) (0.75 mL), mesitylene (0.15 mL) and isoquinoline (0.015 mL). The mixture was sonicated for 2 minutes in order to get a homogenous dispersion and the tube was degassed *via* three freeze-pump-thaw cycles, flame sealed and heated at 120 °C for 4 days. The precipitate was collected by filtration and washed with DMF, EtOH and THF. The resulting solid was dried at 120 °C under vacuum overnight to give 64.7 mg (93 %) of **NDI-COF** as a light brown solid.

-**NDI-CONs**: 1 mg of **NDI-COF** powder was sonicated in 5 mL of milli-Q water for 3 h in an Elmasonic P ultrasonic bath. The resulting colloidal dispersions were centrifuged at 500 rpm for 2 min to eliminate non-exfoliated **NDI-COF**.

- **NDI-polymer**: In a pyrex tube NTCDA (40.7 mg, 0.152 mmol) and TAPB (35.8 mg, 0.102 mmol) were suspended in a mixture of NMP (0.45 mL), mesitylene (0.45 mL) and isoquinoline (0.09 mL). The mixture was sonicated for 2 minutes in order to get a homogenous dispersion and the tube was degassed *via* three freeze-pump-thaw cycles, flame sealed and heated at 120 °C for 4 days. The precipitate was collected by filtration and washed with DMF, EtOH and THF. The resulting solid was dried at 120 °C under vacuum overnight to give 61.7 mg (86 %) of **NDI-polymer** as a dark brown solid.

Electrochemical Methods

- Number of electrons involved in the process. For the determination of the number of electrons involved in the electrochemical process the hydrodynamic voltammograms at an **NDI-CON/GC** disc electrode were recorded at different rotation rates from 100 rpm to 1500 rpm and at the same time the Pt ring currents at 0 V vs. SCE were register (Fig. 3b). The number of electrons involved in the ORR was calculated from equation (S1)

$$n = 4\frac{i_D}{i_{D+\frac{i_R}{N}}} \quad \text{(S1)}$$

where *n* is the number of electrons, *N* is the collection efficiency of the ring (0.218 for the present geometrical arrangement) and i_D and i_R are the measured currents for the disk and ring electrodes, respectively.

- Current stability tests. A constant potential of -0.5 V *vs.* SCE was applied and the current was registered while keeping the rotating electrode spinning at 1500 rpm and immersed in a 0.1 M NaOH O_2 saturated solution.

Theoretical Methods and Structure Modelling

We have carried out a battery of Density Functional Theory (DFT) calculations searching for the optimized ground state geometries of the 2D **NDI-COF** monolayer, as well as its associated 3D crystal structure in different stacking fashions to be directly compared with the experimental evidence.

In a first step, we have performed a preliminary DFT analysis of the two building blocks forming the **NDI-COF** in this study: 1,4,5,8-naphthalenetetracarboxylic dianhydride (NTCDA) and 1,3,5-tris(4-aminophenyl)benzene (TAPB), in order to obtain reasonable starting point geometries towards the assembling of the whole COF system. For that purpose, we have obtained optimized structures of the mentioned isolated gas-phase sub-units by the GAUSSIAN09 code[4] within the B3LYP/cc-pVTZ[5-7] level of theory.

On the basis of the preliminary optimized building blocks we have constructed the periodic model of the 2D structure to be fully optimized with the CASTEP plane-wave DFT code.[8] We have carried out simultaneous full lattice/cell and structure optimizations for the different 2D and 3D **NDI-COF** configurations. The calculations account for an empirical efficient vdW R^{-6} correction (DFT+TS method).[9] We have used the GGA-PBE functional to account for the exchange-correlation (XC) effects[10] and ultra-soft pseudopotentials[11] to model the ion-electron interaction within the H, C, N and O atoms. The Brillouin zones have been sampled by means of optimal Monkhorst-Pack grids.[12] The one-electron wave-functions are expanded in a basis of plane-waves with an energy cut-off of 400 eV for the kinetic energy, which has been adjusted to achieve sufficient accuracy to guarantee a full convergence in total energy and electronic density. All the atomic relaxations were carried out within a conjugate gradient minimization scheme until the maximum force acting on any atom was below 0.02 eV $Å^{-1}$. This simultaneous lattice and structural relaxation protocol provide an optimal strain minimization up to achieve a global stress < 0.01 GPa. Additionally, for the optimized 2D **NDI-COF** we have computed infinite crystal-bulk structures in both the eclipsed stacking (AA) and the staggered stacking (AB) fashions. The theoretical crystal-powder diffractograms have been simulated from the DFT-optimized structures by using the MERCURY package.[13]

Additionally, in order to monitor the evolution of the structure and PXRD features from the eclipsed stacking (AA) to the staggered stacking (AB), we have explored two intermediate stacking possibilities with 1/6 and 1/3 layer offsets. These two intermediate space-filling models

have been DFT-computed within the same theoretical framework abovementioned. It is interesting to mention that these two intermediate interlayer stacking models provide very similar interlayer interaction energies and yield interlayer distances of 3.57 and 3.66 Å, for the 1/6 and 1/3 layer offsets, respectively, to be compared with the values of 3.53 and 3.74 Å for the limiting AA and AB cases, respectively.

Table S1. Screening of conditions for the synthesis of **NDI-COF**.

Solvent: NMP:Mesitylene	**Catalyst: Isoquinoline**	**Concentration (NTCDA+TAPB)**	**Temperature (°C)**	**Activation**	**Crystallinity**
1/1	5 %	20 mg/mL	150	Vacuum	No
5/1	2 %	40 mg/mL	150	Vacuum	No
7/1	2 %	40 mg/mL	120	Vacuum	No
7/1	10 %	40 mg/mL	120	Vacuum	No
1/1	5 %	80 mg/mL	200	Vacuum	No
1/1	2 %	80 mg/mL	200	Vacuum	No
1/1	5 %	80 mg/mL	150	Vacuum	No
1/1	2 %	80 mg/mL	150	Vacuum	No
1/1	10 %	80 mg/mL	120	Vacuum	No
1/1	2 %	80 mg/mL	120	Vacuum	No
7/1	10 %	80 mg/mL	120	Vacuum	No
7/1	2 %	80 mg/mL	120	Vacuum	No
5/1	10 %	80 mg/mL	120	Vacuum	Low
5/1	2 %	80 mg/mL	120	Vacuum	Moderate
5/1	1 %	80 mg/mL	120	Vacuum	Moderate
5/1	2 %	80 mg/mL	120	$scCO_2$	High

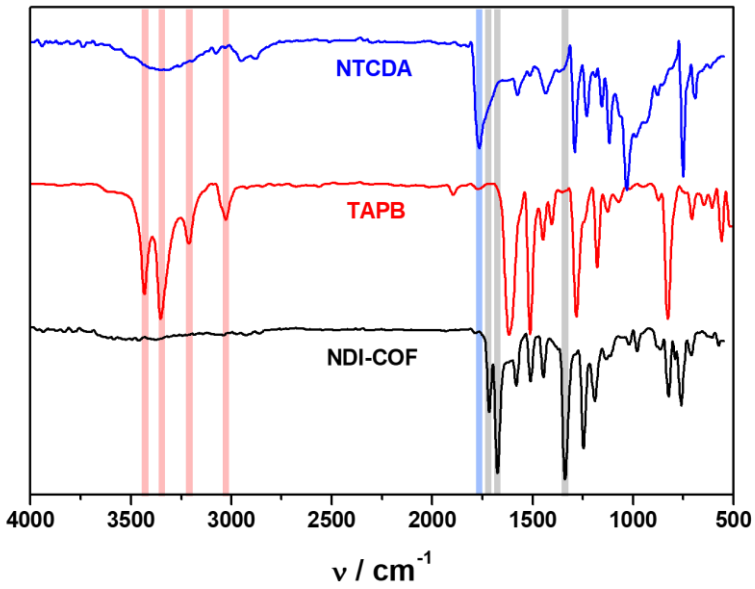

Figure S1. FTIR spectra of NTCDA (blue), TAPB (red) and **NDI-COF** (black) highlighting the C=O band from NTCDA (light blue), the N-H bands from TAPB (light red) and the six-membered imide ring bands from **NDI-COF** (light grey).

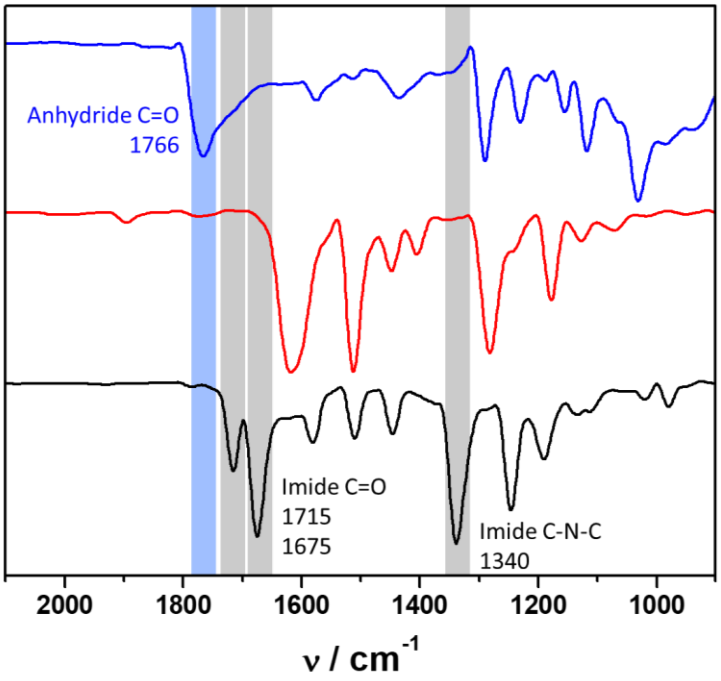

Figure S2. Zoomed section of the FTIR spectra of NTCDA (blue), TAPB (red) and **NDI-COF** (black) highlighting the C=O band from NTCDA (light blue) and the six-membered imide ring bands from **NDI-COF** (light grey).

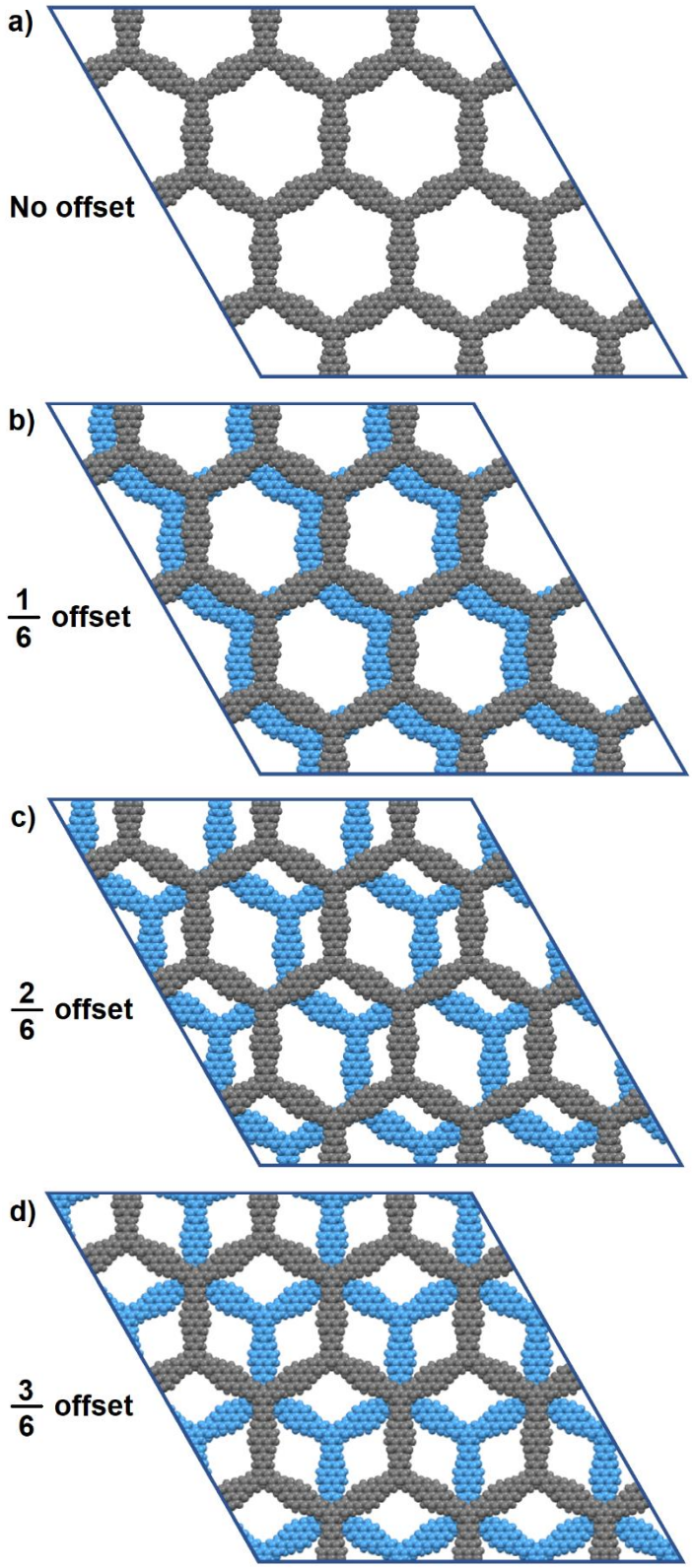

Figure S3. Space filling modelled structures of **NDI-COF** in the eclipsed AA stacking mode (a), with a 1/6 layer offset (b), with a 1/3 layer offset (c) and in the staggered AB stacking mode (d).

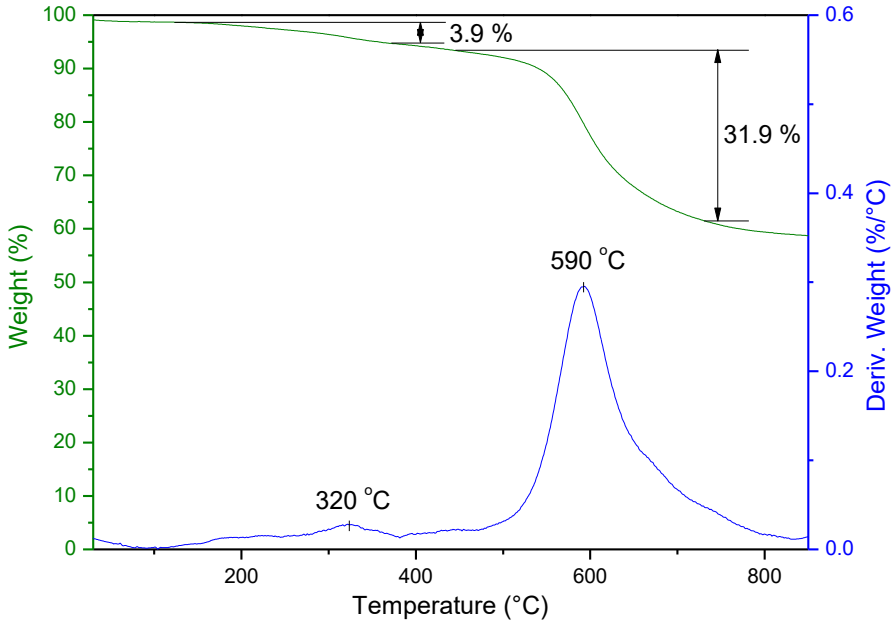

Figure S4. TGA curve of **NDI-COF**.

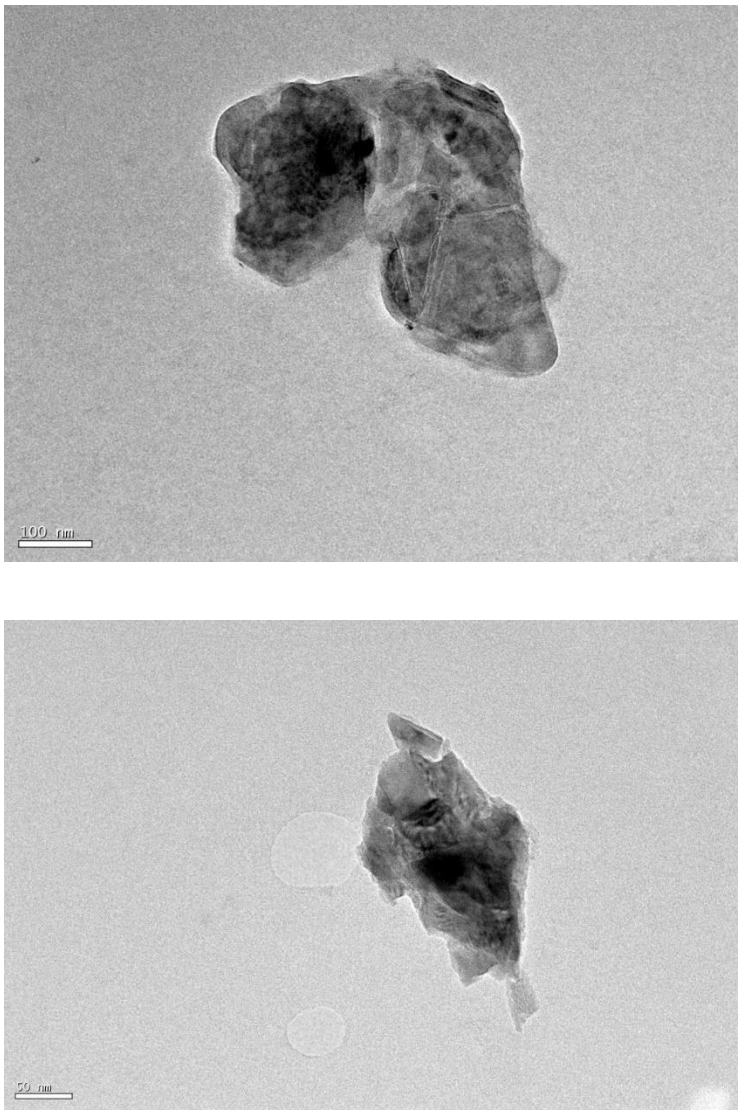

Figure S5. TEM images of **NDI-CONs**.

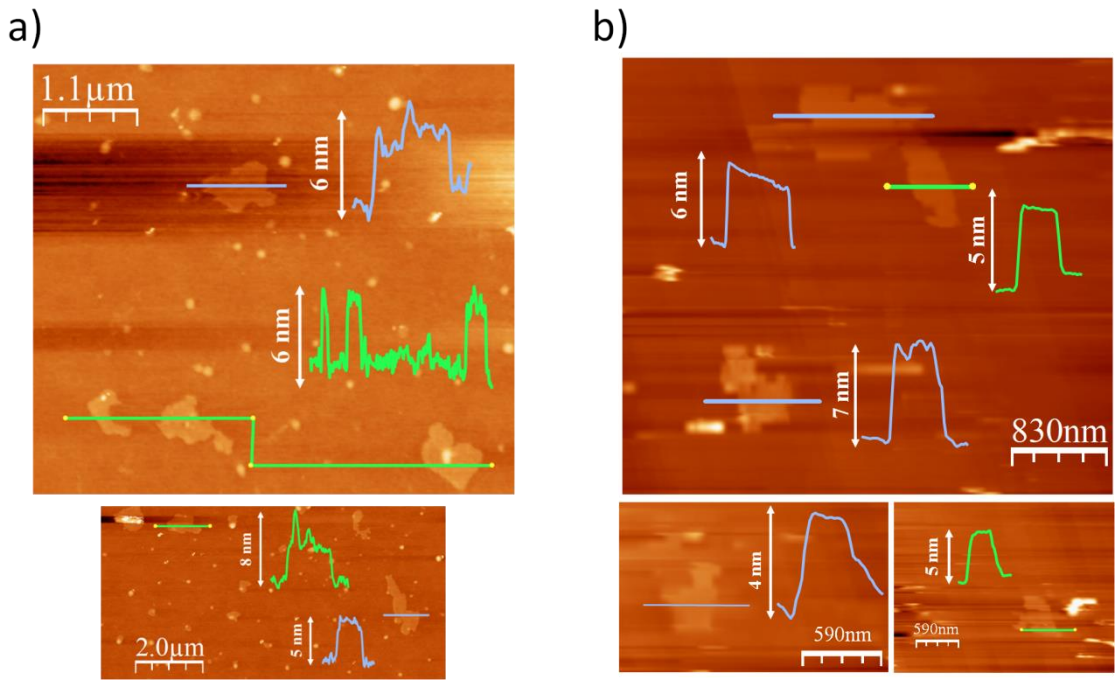

Figure S6. AFM topographic images of exfoliated **NDI-CONs** on HOPG and their height profiles along the corresponding lines. a) Before and b) after operating for 10000 s in a 0.1 M NaOH O_2 saturated solution at a constant potential of - 0.5 V vs. SCE.

Statistic Height Profile analysis carried out in 25 **NDI-CONs** before and after operating for 10000 s confirms that there are no appreciable changes (Height before: 4.8 ± 0.2 nm, after: 5.0 ± 0.3 nm).

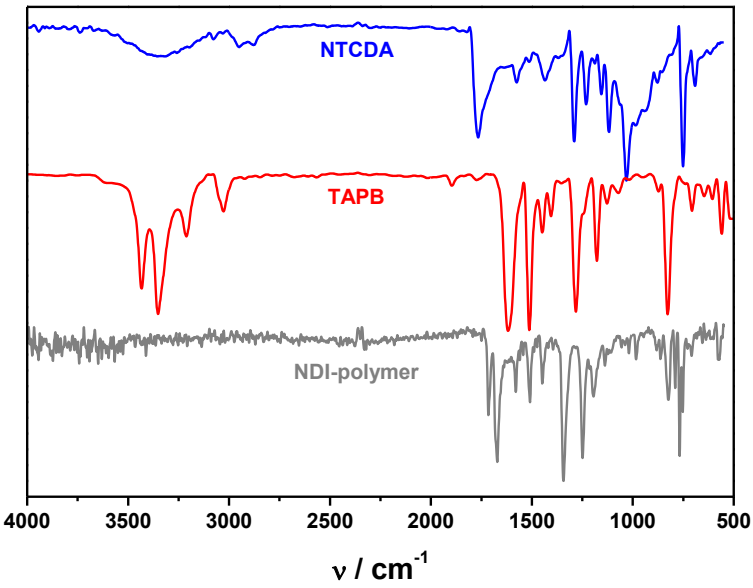

Figure S7. FTIR spectra of NTCDA (blue), TAPB (red) and **NDI-polymer** (black).

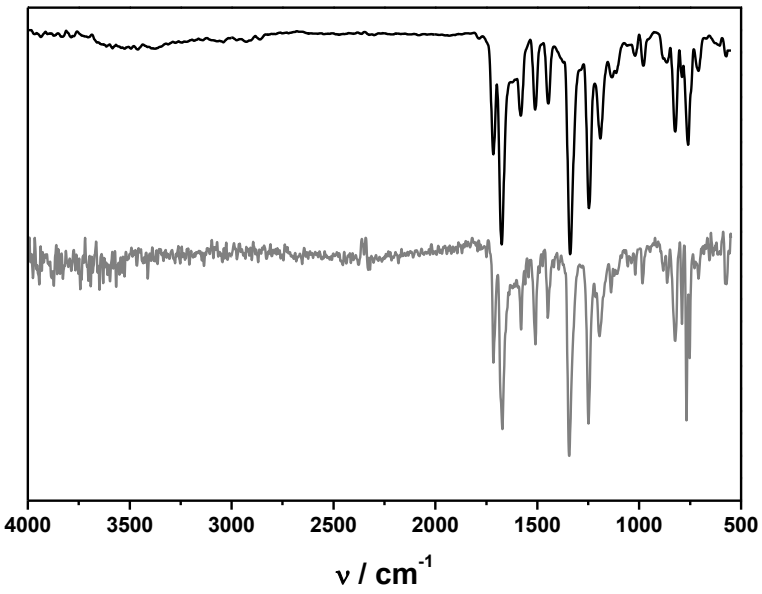

Figure S8. Comparative FTIR spectra of **NDI-COF** (black) and **NDI-polymer** (grey).

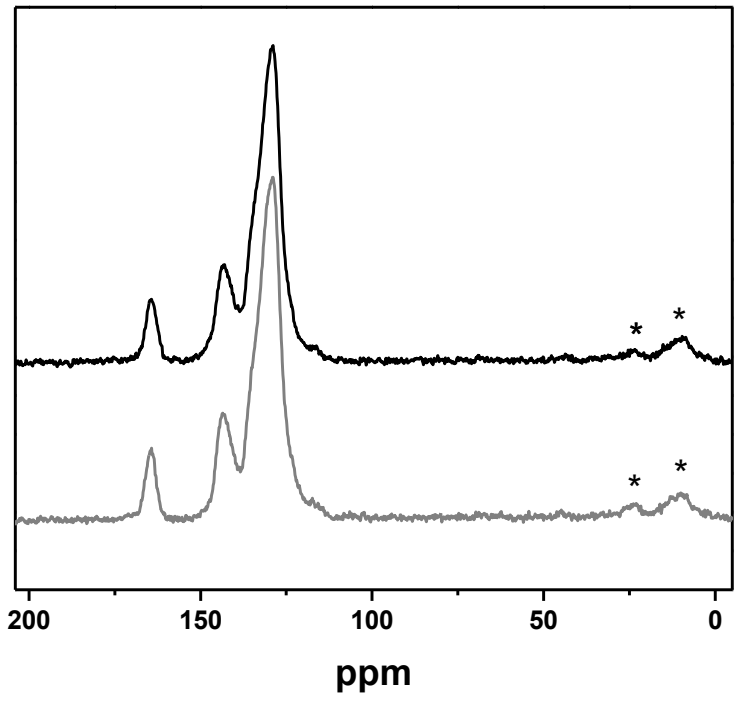

Figure S9. Comparative ^{13}C-CP/MAS-NMR spectra of **NDI-COF** (black) and **NDI-polymer** (grey). Asterisks indicate spinning side bands.

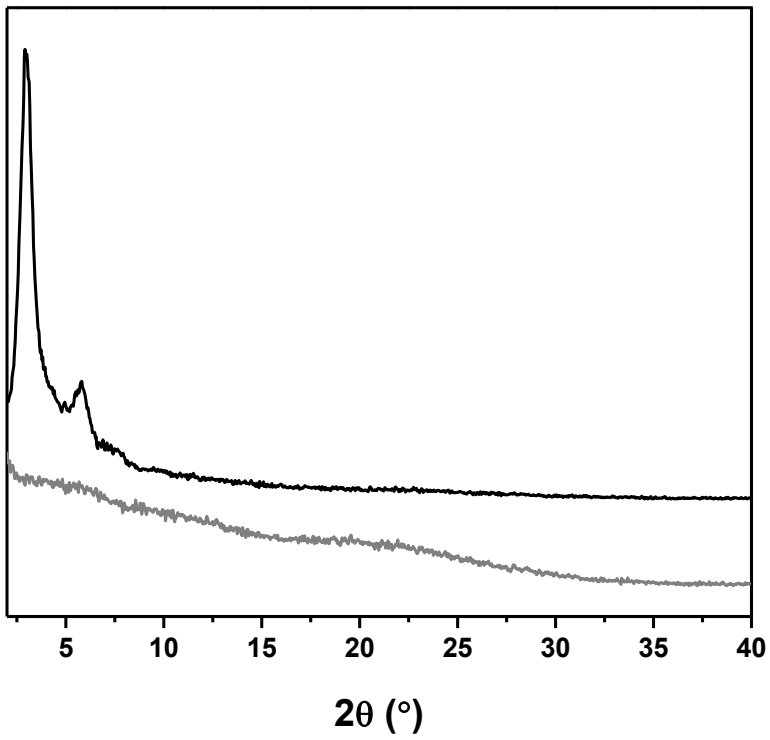

Figure S10. Comparative PXRD patterns for **NDI-COF** (black) and **NDI-polymer** (grey).

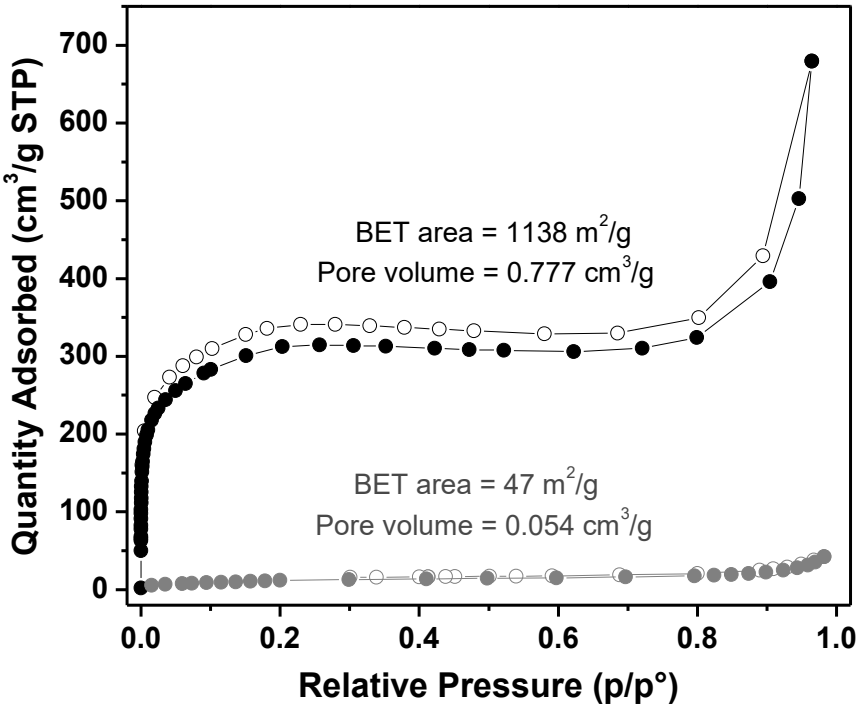

Figure S11. Comparative N_2 (77 K) sorption isotherms for of **NDI-COF** (black) and **NDI-polymer** (grey).

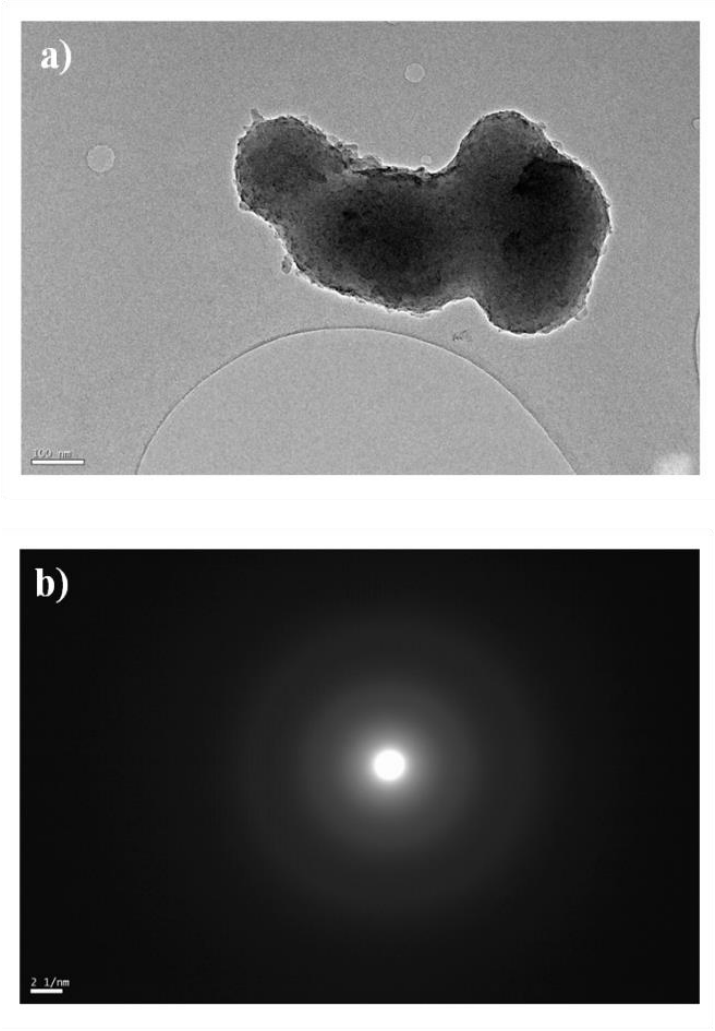

Figure S12. a) TEM image of **NDI-polymer** and b) its SAED analysis.

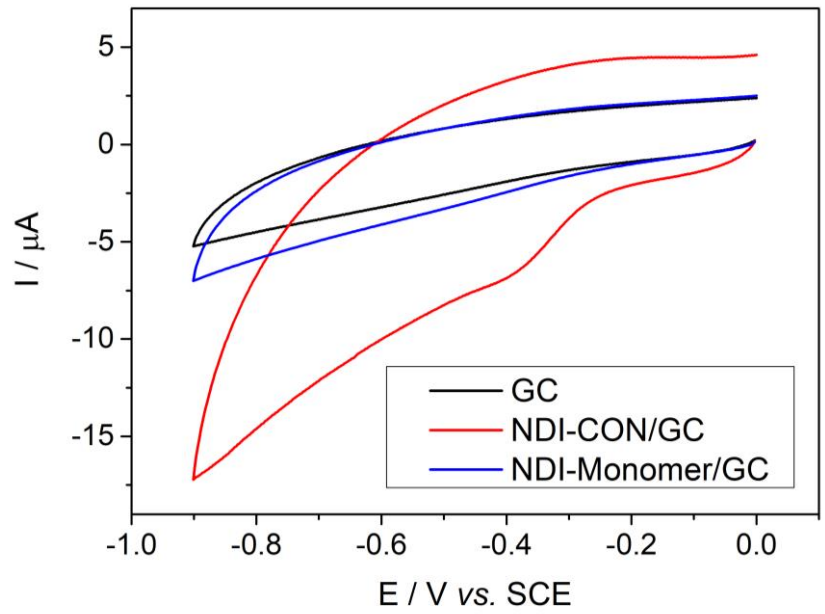

Figure S13. Cyclic Voltammetry of a GC electrode (black), **NDI-CON/GC** electrode (red) and a **NDI-Monomer/GC** electrode (blue) in 0.1 M NaOH N_2 saturated solution.

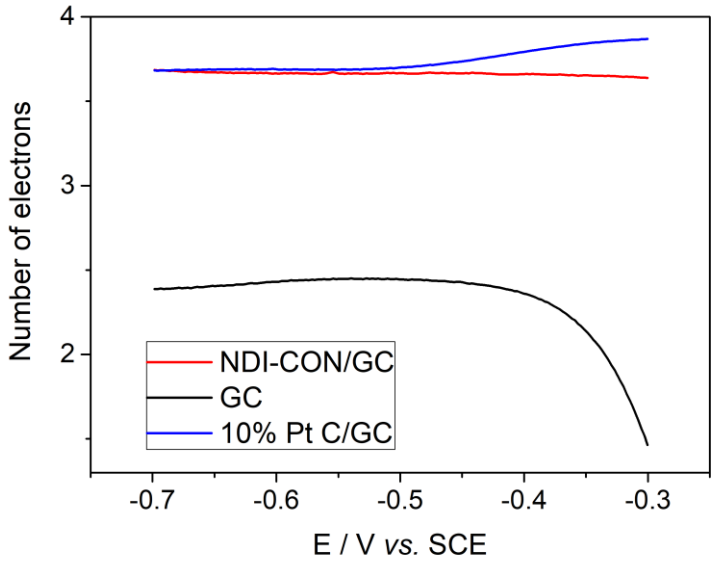

Figure S14. Number of electrons calculated for ORR using RRDE at different potentials at 10% Pt C/GC disc electrode (blue), GC disc electrode (red) and **NDI-CON/GC** disc electrode (black).

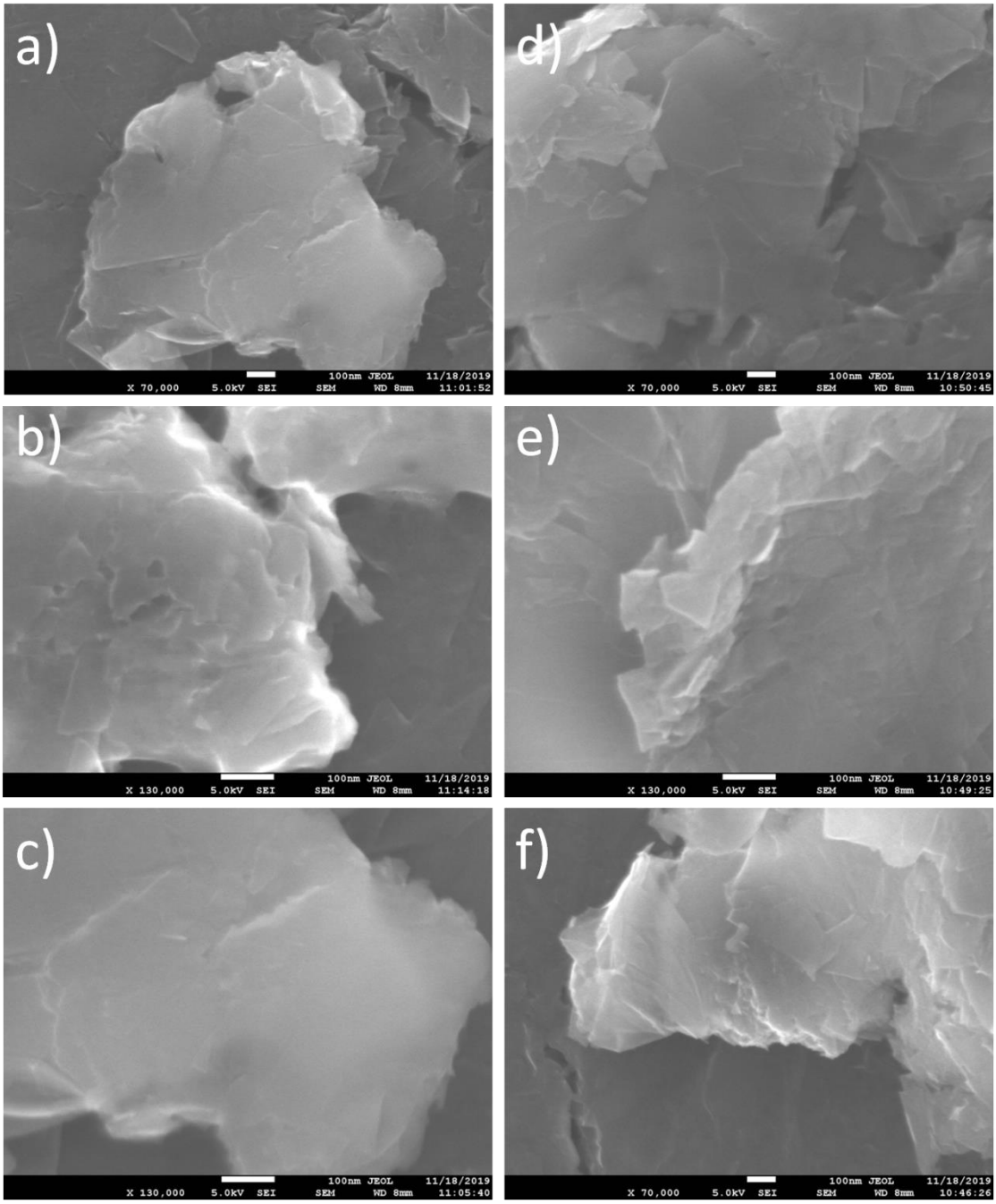

Figure S15. SEM images of **NDI-CONs** before (a-c) and after (d-f) operating for 10000 s in a 0.1 M NaOH O_2 saturated solution at a constant potential of - 0.5 V vs. SCE.

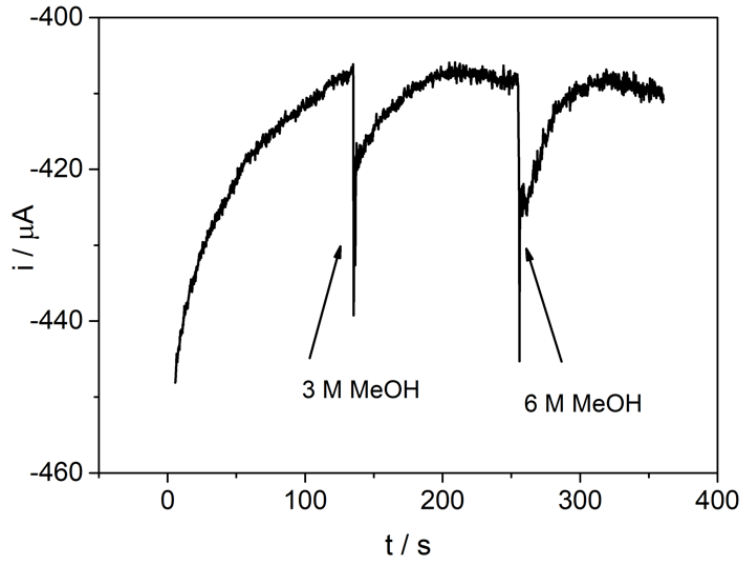

Figure S16. MeOH interference study of **NDI-CON/GC** electrode operating at a constant potential (- 0.5 V vs. SCE) in 0.1 M NaOH O_2 saturated solution.

References

1 A. de la Peña Ruigómez, D. Rodríguez-San-Miguel, K. C. Stylianou, M. Cavallini, D. Gentili, F. Liscio, S. Milita, O. M. Roscioni , M. L. Ruiz-González, C. Carbonell, D. Maspoch, R. Mas-Ballesté, J. L. Segura and F. Zamora, *Chem. Eur. J.*, 2015, **21**, 10666-10670.

2 S. Guo, W. Wu, H. Guo and J. Zhao, *J. Org. Chem.*, 2012, **77**, 3933-3943.

3 I. Horcas, R. Fernández, J. M. Gómez-Rodríguez, J. Colchero, J. Gómez-Herrero and A. M. Baro, *Rev. Sci. Instrum.*, 2007, **78**, 013705.

4 M. J. Frisch, G. W. Trucks, H. B. Schlegel, G. E. Scuseria, M. A. Robb, J. R. Cheeseman, G. Scalmani, V. Barone, B. Mennucci, G. A. Petersson, H. Nakatsuji, M. Caricato, X. Li, H. P. Hratchian, A. F. Izmaylov, J. Bloino, G. Zheng, J. L. Sonnenberg, M. Had and D. J. Fox, Gaussian 09, Revision A.01, 2009.

5 A. D. Becke, *J. Chem. Phys.*, 1993, **98**, 5648-5652.

6 P. J. Stephens, F. J. Devlin, C. F. Chabalowski and M. J. Frisch, *J. Phys. Chem.*, 1994, **98**, 11623-11627.

7 T. H. Dunning, *J. Chem. Phys.*, 1989, **90**, 1007-1023.

8 J. Clark Stewart, D. Segall Matthew, J. Pickard Chris, J. Hasnip Phil, I. J. Probert Matt, K. Refson and C. Payne Mike, *Z. Kristallogr. Cryst. Mater.*, 2005, **220**, 567-570.

9 A. Tkatchenko and M. Scheffler, *Phys. Rev. Lett.*, 2009, **102**, 073005.

10 J. P. Perdew, K. Burke and M. Ernzerhof, *Phys. Rev. Lett.*, 1996, **77**, 3865-3868.

11 D. Vanderbilt, *Phys. Rev. B*, 1990, **41**, 7892-7895.

12 J. D. Pack and H. J. Monkhorst, *Phys. Rev. B*, 1977, **16**, 1748-1749.

13 P. R. Edgington, P. McCabe, C. F. Macrae, E. Pidcock, G. P. Shields, R. Taylor, M. Towler and J. Van De Streek, *J. Appl. Cryst.*, 2006, **39**, 453-457.